Supplemental material

Medeiros et al., https://doi.org/10.1083/jcb.201801168

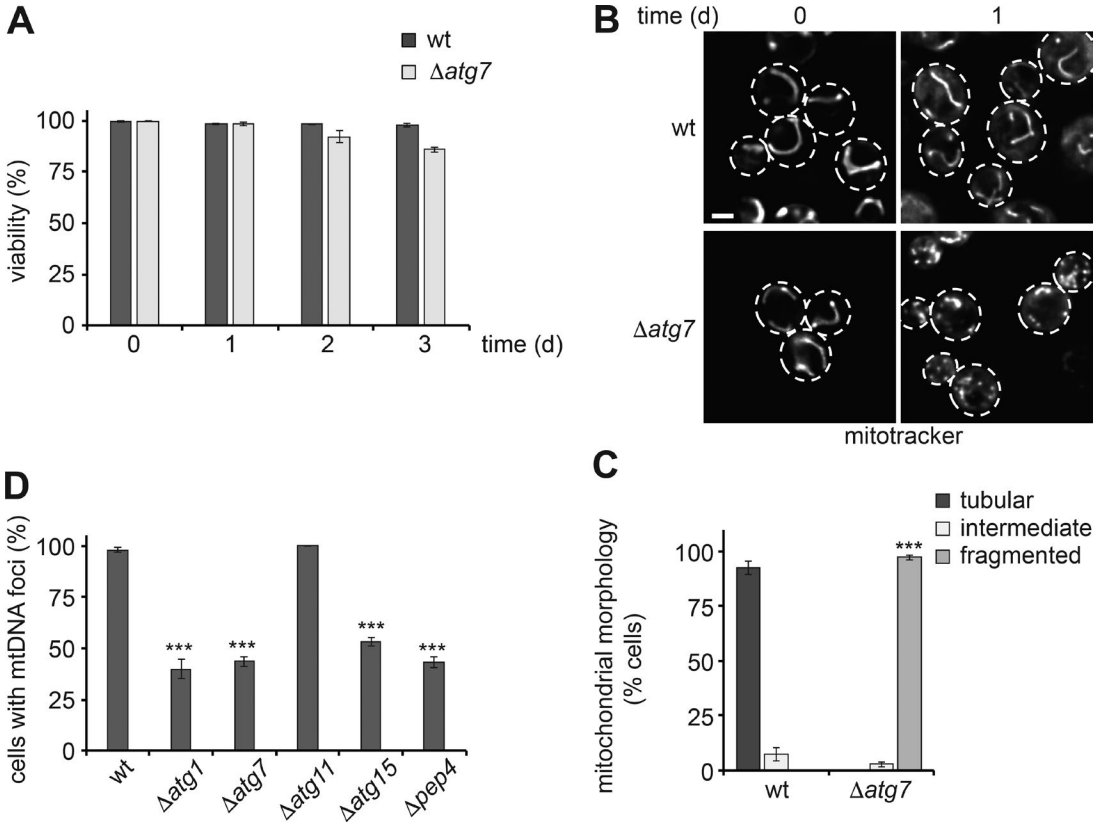

Figure S1. **mtDNA maintenance and mitochondrial morphology, but not cell viability, depend on general autophagy. (A)** Viability of WT and Δ*atg7* cells was analyzed at indicated time points using phloxine B staining and flow cytometry. Data are means ± SD (n = 3; 10^5 events/sample). **(B and C)** Mitochondrial morphology was examined in WT and Δ*atg7* cells using MitoTracker and fluorescence microscopy at indicated time points. **(B)** Representative single section images are shown. **(C)** Quantitative classification of mitochondrial morphologies as shown in B. Data are means ± SD (n = 3; 150 cells). **(D)** mtDNA maintenance in WT, Δ*atg1*, Δ*atg7*, Δ*atg11*, Δ*atg15*, and Δ*pep4* cells performed as described in Fig. 1 (C and D). Data are means ± SD (n = 3; ≥75 cells). Dashed lines indicate cell boundaries. Bars, 2 µm. *t* tests: ***, P < 0.001.

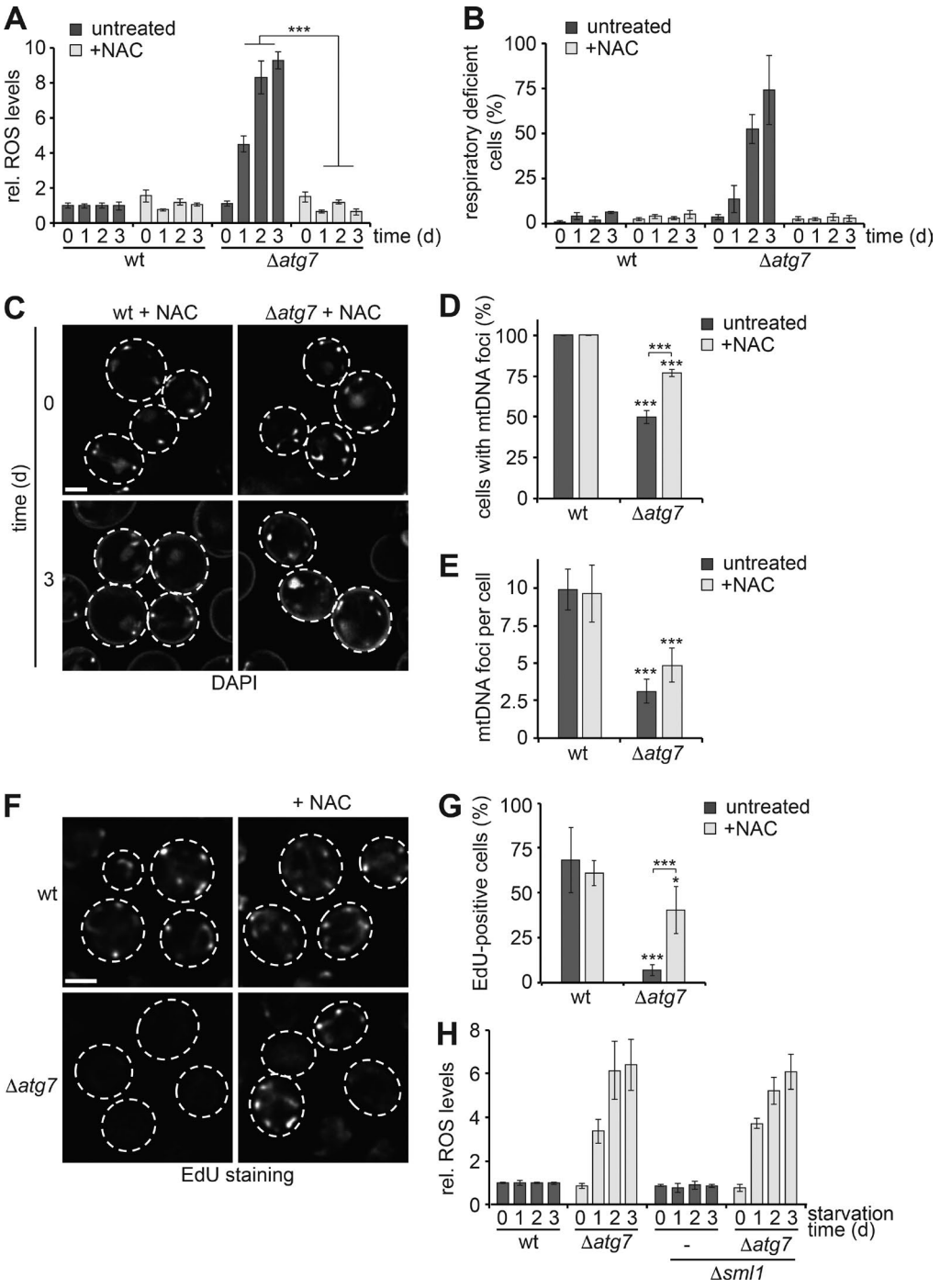

Figure S2. **NAC treatment alleviates ROS production, loss of respiratory competence, and defective mtDNA synthesis and maintenance in autophagy-deficient cells. (A)** NAC treatment prevents elevated ROS levels in Δ*atg7* cells. WT and Δ*atg7* cells were grown to log-phase (0 d) or shifted to starvation medium ± NAC and analyzed for ROS levels using DHE staining and flow cytometry at indicated time points. Data are means ± SD (n = 3). **(B)** Respiratory competence in Δ*atg7* cells upon regrowth after starvation ± NAC. WT and Δ*atg7* cells were plated on YPD plates to test for respiratory competence based on red/white selection at indicated time points during starvation. Data are means ± SD (n = 3). **(C–E)** mtDNA maintenance in autophagy-deficient cells in dependence of ROS production. WT and Δ*atg7* cells were grown to log-phase and shifted to starvation medium ± NAC. mtDNA foci were visualized by DAPI staining and in vivo fluorescence imaging at indicated time points. **(C)** Representative single section images are shown. **(D and E)** Quantification of cells with mtDNA foci (D) or the number of mtDNA foci in foci-positive cells (E). Data are means ± SD (n = 3; ≥75 cells). **(F and G)** NAC treatment alleviates the defects in mtDNA synthesis in autophagy-deficient cells during starvation. WT and Δ*atg7* cells were grown to log-phase and shifted to starvation medium ± NAC for 3 h and subsequently exposed to EdU for 24 h. EdU incorporation in fixed cells was visualized by the use of Alexa Fluor 647, copper click chemistry, and fluorescence imaging. **(F)** Representative single section images after visualization of EdU incorporation in WT and Δ*atg7* during starvation ± NAC (1 d). **(G)** Quantification of mtDNA synthesis in WT and Δ*atg7* cells of cells shown in E. Data are means ± SD (n ≥ 3; 150 cells). **(H)** WT, Δ*sml1*, Δ*atg7*, and Δ*sml1*Δ*atg7* cells were grown in log-phase (0 d) or shifted to starvation medium and analyzed for ROS levels using DHE staining and flow cytometry at indicated time points. Data are means ± SD (n = 3). Dashed lines indicate cell boundaries. Bars, 2 µm. *t* tests: *, P < 0.05; ***, P < 0.001. Rel., relative.

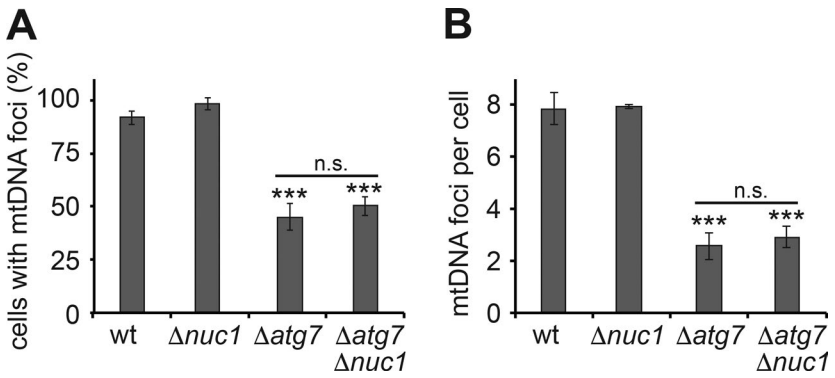

Figure S3. **EndoG (Nuc1) does not affect mtDNA maintenance during starvation. (A and B)** WT, Δ*nuc1*, Δ*atg7*, and Δ*atg7*Δ*nuc1* cells were grown to log-phase and shifted to starvation medium. mtDNA foci were visualized by DAPI staining and analyzed by in vivo fluorescence imaging at indicated time points. Quantifications of cells with mtDNA foci (A) or the number of mtDNA foci in foci-positive cells (B). Data are means ± SD (n = 3; ≥75 cells). *t* tests: ***, P < 0.001; n.s., not significant.